Transport mechanism of Γ- and X-band electrons in $Al_xGa_{1-x}As$/AlAs/GaAs double-barrier quantum-well infrared photodetectors

T. Osotchan,* V. W. L. Chin,† and T. L. Tansley

Semiconductor Science and Technology Laboratories, Macquarie University, New South Wales 2109, Australia

(Received 26 March 1996)

The effect of the Γ- and X-band electrons in the $Al_{0.25}Ga_{0.75}As$/AlAs/GaAs double-barrier quantum well (DBQW) is investigated by a microscopic empirical pseudopotential calculation. The DBQW structure used in the calculation is designed as a 3–5-μm quantum-well infrared photodetector with an associated transition energy of 313 meV. DBQW tunneling transmission via Γ- and X-like states as a function of electron energy and applied voltage are described and compared to that in a single-barrier AlAs/GaAs quantum well. The dark current is simulated by the confined ground-state electron tunneling out of the well. We find that, at high-bias voltage, tunneling via X-like states increases the current by a few orders of magnitude. We have also varied the additional barrier thickness and found that for a very thin (<20 Å) additional barrier DBQW, the excited-state electrons are not blocked by the Γ-band barrier, and may give a high photocurrent without the assistance of the X band, although the dark current also increases. [S0163-1829(96)01527-5]

I. INTRODUCTION

Quantum-well (QW) structures based on intersubband transitions between confined states in the well-established $Al_xGa_{1-x}As$/GaAs system have been studied intensively for quantum-well infrared photodetector (QWIP) applications.[1] For a simple $Al_xGa_{1-x}As$/GaAs square well, the response wavelength associated with the state energy difference can be designed only to the limit of 5.6 μm at the Γ-X crossover composition of the $Al_xGa_{1-x}As$ barrier.[2] With additional thin AlAs barriers on both sides of the GaAs well, however, the double-barrier quantum-well (DBQW) response can be extended to shorter infrared wavelengths in the 3–5-μm band.[3–5] The ultrathin and high Al content layers not only push the excited-state energy higher, but also allow photoexcited carriers to tunnel through easily while ground-state tunneling is suppressed by the combined higher and lower $Al_xGa_{1-x}As$ barriers. The dark current for the bound-to-quasibound QWIP's is therefore significantly reduced.[1,6]

Although the full, indirect AlAs barrier can be reduced to a minimum thickness, the influence of the X band on the DBQW is evident.[6–8] We have therefore theoretically investigated the effects of the X path on electron transport in the DBQW structure, and compared the result to that in a full AlAs barrier QW. The nominal profiles are shown in Fig. 1. The effects of single and double-barrier resonant tunneling structures on X-band channels through which electrons can tunnel out of the well will first be described.

For an AlAs/GaAs single barrier, X-band electron tunneling dominates when the barrier is thicker than 40 Å.[9] For an $Al_xGa_{1-x}As$ barrier, with x increasing from 0.3 to 0.8, the effective mass derived from the tunneling current increases from the Γ-valley electron mass to the transverse X-valley electron mass (0.2).[10] Due to the presence of a quasibound state associated with the X valley in the single barrier, negative differential resistance can be observed.[11,12] In a hydrostatic pressure measurement, the differential current peak shifts linearly downward with voltage, and is estimated to lie at zero voltage when the pressure brings the Γ(GaAs)-X(AlAs) offset to zero.[13,14] Transport through various channels, such as Γ-Γ-Γ, Γ-X-Γ, and Γ-X-X, have been used to demonstrate the current source.[9,11,12,14–17]

In the DBQW structure, calculations including X-like state tunneling give higher valley currents than the single-

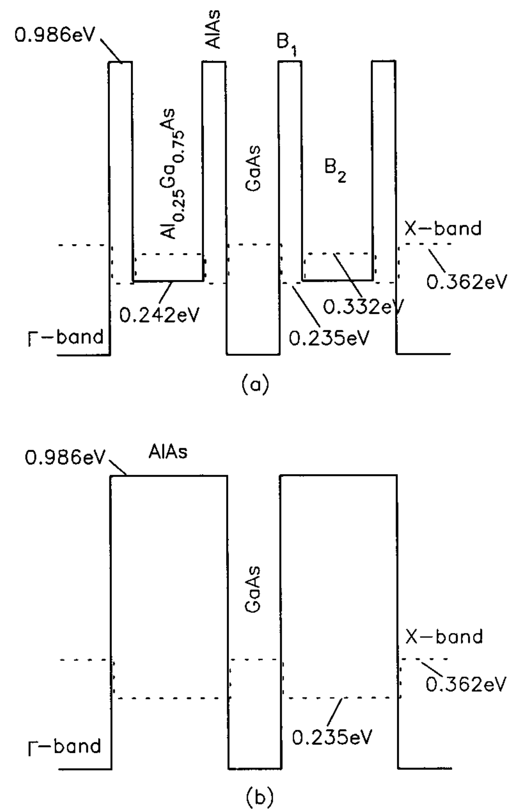

FIG. 1. Γ (solid line) and X (dotted line) conduction-band profiles for (a) an $Al_{0.25}Ga_{0.75}As$/AlAs/GaAs DBQW and (b) an AlAs/GaAs QW.

 © 1996 The American Physical Society

band calculation, leading to a more realistic peak-to-valley ratio.[18,19] The negative resistance associated with X-like states has also been observed in narrow GaAs layer structures in which the Γ-like quasibound state is higher than the X-like state,[11] while hydrostatic pressure can also lower the X-like quasibound states confined in the AlAs layer.[20] A number of tunneling paths, such as Γ-X-Γ-X-Γ (Ref. 21) and Γ-X-X-X-Γ,[22] have been considered.

X-band electron tunneling through the Γ-band barrier has also been studied in a triple barrier. It has been found that the GaAs layer can be used as the X-band barrier when its thickness is less than 30 Å.[23] Sequential tunneling current was observed in a superlattice designed with the X level between the ground and first excited states, so that, when a voltage is applied, electrons from the ground state in one well tunnel to the X level in the barrier, and then to the Γ-like ground state in the next well sequentially.[24]

Both the microscopic empirical pseudopotential technique[25–30] and the empirical tight-binding method[17–19,22,31,32] have been used to calculate transmission over a number of valleys and bands. Envelope-function approximations with intervalley and/or interband parameters obtained from either the pseudopotential[33,34] or tight-binding band[35,36] have been employed to include the effects of other bands. Transfer-matrix, or rather a scattering matrix which reduces the unstable numerical error in the transfer matrix,[28] and Green's-function[17] methods are usually utilized to calculate the transmission probability through the heterostructure.

In order to incorporate the influence of other valleys, we have therefore used an empirical psuedopotential technique with a scattering matrix to probe the effects of X-electron transport in the DBQW. This is because the pseudopotential method, with plane-wave basic wave functions, can directly deal with the aperiodic structure with both unbound and quasibound states in a DBQW. This we compare with the full indirect barrier QW. Due to the complication of the full band implementation, the self-consistent potential with the doped layers was neglected, and a flat-band condition was assumed. The calculation method is briefly reviewed in Sec. II. The X-band contribution to the QWIP dark current for the $Al_{0.25}Ga_{0.75}As$/AlAs/GaAs DBQW and a comparison with the AlAs/GaAs QW is elaborated upon in Sec. III.

II. CALCULATION METHOD

An empirical pseudopotential complex-band-structure method was used to calculate the electronic wave functions in each layer, which were then connected throughout the heterostructure by the scattering matrix. The wave function of the system $[\Psi^n(\mathbf{r})]$ at energy E in a semiconductor layer (n) is written as a linear combination of the known pseudopotential bulk basis states (ϕ_j^n) within this energy[30]

$$\Psi^n(\mathbf{r})=\sum_{j=1}^{2N}\Phi_j^n=\sum_{j=1}^{2N}a_j^n\phi_j^n=\sum_{j=1}^{2N}a_j^n\sum_{\mathbf{g}}b_{\mathbf{g}}e^{i(\mathbf{k}_j^n+\mathbf{g})\cdot\mathbf{r}},\tag{1}$$

where $\mathbf{g}$ is a reciprocal-lattice vector summed over three-dimensional reciprocal lattices, $\mathbf{k}_j^n$ are the bulk wave vectors, and $b_{\mathbf{g}}$ are the normalized bulk basic state coefficients. The $2N$ selected bulk states (one set of N states for the left-to-right wave functions, and the other set of N for the right-to-left wave functions) include both the usual propagating Bloch states (real $\mathbf{k}_j^n$) and the evanescent states (complex $\mathbf{k}_j^n$). Since the bulk periodicity parallel to the interface plane is assumed to be continuous throughout the heterostructure, only the wave vector perpendicular to the surface remains. By matching the wave functions and their derivatives at the interface planes, the equality of the two-dimensional reciprocal vector coefficients can be written into a matrix form.[30] Use of the stable scattering matrix method[28] allows the matrix to be rearranged and separated into incoming and outgoing wave-function matrices.

In order to determine the transmission probability, all incoming state coefficients both in the first and last layers are set to zero, with the exception of one of the specified incident state coefficients in the first layer, which is set to unity. The incident state can be set to be either a Γ- or X-valley electron state. The outgoing state coefficients for the first and last layers correspond to the reflection (R) and transmission (T) probabilities, respectively. R and T were calculated from the definition of the current flux[29]

$$R=\frac{J_{\text{reflect}}}{J_{\text{incident}}},\quad T=\frac{J_{\text{transmit}}}{J_{\text{incident}}},\tag{2}$$

where $J_x=\text{Re}[\Phi_x^*(-i\nabla\Phi_x)]$. The R and T for each wave vector (i.e., Γ- or X-like states) can be calculated separately by the above definition, and the summation of all transmitted components becomes the total transmission.

As an applied voltage dropped across the layer, each layer is divided into many small sections and treated as a series of layers with all material parameters the same, except for their potentials. By the same procedure, the transmission as a function of applied voltage can be calculated with the number of sections limited only by the computational time demands.

We assumed that the major dark current in the QWIP originates principally from the two-dimensional electron-tunneling current from the doped well.[37] The effective number of electrons thermally excited out of the well is proportional to the product of the two-dimensional density of states in the well, the transmission probability through the QW barrier $[T(E,V)]$, and the Fermi distribution at the ambient temperature. By approximating the density of states of the infinite well, the current density (j) which accounts for both thermionic emission and thermionic-assisted tunneling can be written as[38]

$$j=\left(\frac{em^*}{\pi\hbar^2 l}\right)v(V)\int_{E_{\Gamma0}}^{\infty}\frac{T(E,V)}{1+e^{(E-E_{\Gamma0}-E_F)/k_BT}}\,dE,\tag{3}$$

where l is the length of well width and barrier thickness, V is the voltage drop across the QW barrier, and E_F is the Fermi energy in the QW with respect to the ground-state energy $(E_{\Gamma0})$. The collector velocity $[v(V)]$ was calculated by an empirical formula $v(V)=\mu F/\sqrt{1+(\mu F/v_s)^2}$, where F is the electric field, μ is the mobility, and v_s is the saturation velocity.

III. RESULTS AND DISCUSSION

The transmission for the $Al_{0.25}Ga_{0.75}As$/AlAs/GaAs DBQW was calculated as a function of energy and applied

voltage and compared to the AlAs/GaAs QW. The local pseudopotential parameters for GaAs and AlAs are as given by Ref. 39. In this work, 27 plane waves have been used in the complex-band-structure calculation. It should be emphasized that using additional plane waves does not make any significant difference, for example, in a 65-plane-wave calculation the effective masses are modified by only about 3%, at the expense of more than an order of magnitude increase in computational time.[30] The parameters for $Al_xGa_{1-x}As$ alloys are linear interpolations of the binary compounds. The heterostructure conduction-band offset is evaluated as 65% of the Γ-band energy-gap difference between the two adjacent semiconductors, and the other material parameters are obtained from Adachi.[40] A typical DBQW structure for 3–5-μm response wavelength consisting of a 45-Å GaAs well, a 20-Å $Al_{0.25}Ga_{0.75}As$ additional barrier (B_1), and a 60-Å $Al_{0.25}Ga_{0.75}As$ barrier (B_2) is specified for this calculation. The energy-band offsets showing both the Γ and X bands and their relative energies for the DBQW structure studied are given in Fig. 1(a). The full barrier QW with the same overall dimensions, that is a 100-Å AlAs barrier and a 45-Å GaAs well, which we calculated for comparison, is shown in Fig. 1(b).

With the difficulty in accurately describing experimentally determined electronic structure with empirical band structure, the offset energy values calculated (Fig. 1) from the given parameters are shifted from the experimentally accepted values. The experimental Γ-X splitting energies in GaAs and AlAs are 0.46 (Ref. 41) and 0.90 eV,[42] respectively. These are larger than the calculated values of 0.36 and 0.75 eV (see Fig. 1). The direct conduction-band offset between GaAs and AlAs layers was determined at the value of 1.06 eV,[43] which is also larger than the value from Fig. 1 (0.99 eV). This will result in a systematic shift in the energy of the transmission spectra, but we believe that the general feature and the conclusions drawn on the Γ- and X-band electron transport are still significant and valid. However, with an inaccuracy in the energy-band parameters, the energy levels reported need to be adjusted by an appropriate factor.

A. Zero-bias-voltage structures

In order to investigate the electron tunneling and quasibound characteristics, the transmission probabilities through the QW barrier and the whole finite barrier QW structures as a function of the incident Γ electron energy (E) were calculated, and are shown in Fig. 2. By way of example, the transmission through the 100-Å-thick AlAs barrier in Fig. 2(a) is used to illustrate the tunneling out of an AlAs/GaAs QW. The Γ-valley incident electron at energy lower than the AlAs X-minimum ($E<0.235$ eV) tunnels via the Γ-Γ-Γ path. The transmission here is very low because of the height and thickness of the AlAs Γ-band barrier. When the Γ-valley electron energy is higher than the AlAs X minimum, but lower than the GaAs X minima ($0.235<E<0.362$ eV), the electron may tunnel via the X-like state in the AlAs layer (Γ-X-Γ). This results in an abrupt jump in transmission at 0.235 eV, about ten orders of magnitude in this case. Since the X-valley effective mass is heavy and the X-like well is very wide (100 Å), a series of transmission peaks corresponding to the quasibound states in the AlAs X-like well appears in this energy region.

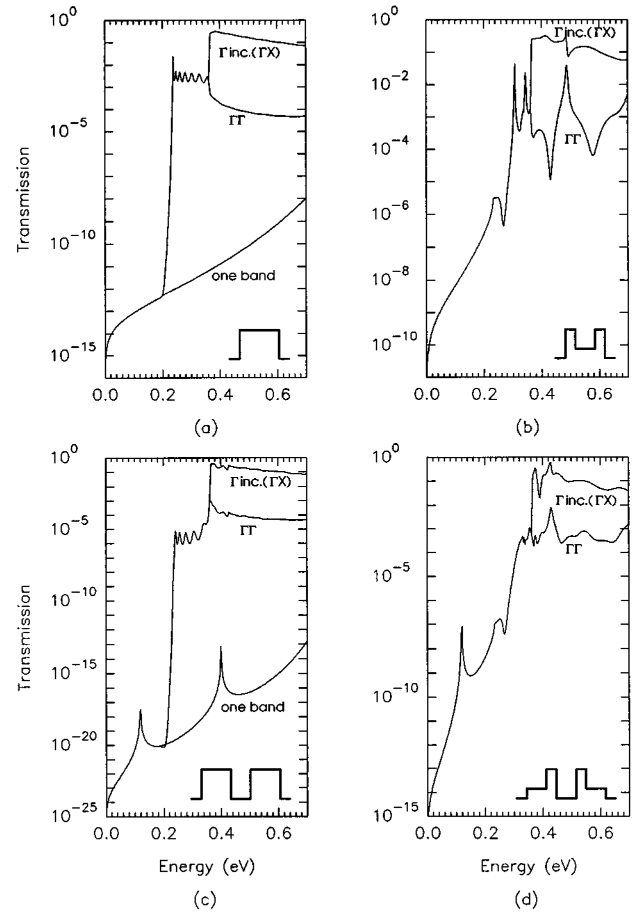

FIG. 2. Γ-valley incident electron transmission (Γinc.) including one-band, ΓΓ, and ΓX components as a function of energy for (a) 100-Å AlAs single barrier, (b) 20-Å AlAs, 60 Å $Al_{0.25}Ga_{0.75}As$, and 20-Å AlAs DBQW barrier, (c) 80-Å AlAs, 45-Å GaAs, and 80-Å AlAs QW's, and (d) 60-Å $Al_{0.25}Ga_{0.75}As$, 20-Å AlAs, 45-Å GaAs, 20-Å AlAs, and 60-Å $Al_{0.25}Ga_{0.75}As$ DBQW structures. In each case the inset shows the Γ-barrier profile.

Above 0.362 eV the incident Γ-valley electron in the GaAs layer at one side may transfer to the X valley at the other side (ΓX) via either the Γ or X valley in the AlAs layer (Γ-Γ-X or Γ-X-X). Two transmission probability types are displayed in Fig. 2: the ΓΓ and total transmission (Γinc.). In most cases, since the ΓX transmission is much greater than ΓΓ (about three orders in this case), the ΓX transmission is close to providing the total transmission above 0.362 eV. In order to show the tunneling process without the assistance of the X-like state, the one-band transmission calculated by using only one Γ-like $\mathbf{k}$ state ($N=1$) was also evaluated and is shown in Fig. 2. For $E>0.235$ eV the one-band transmission is lower than the ΓΓ transmission (X-like-state-assisted tunneling), and even much lower than the ΓX transmission when $E>0.362$ eV.

The electron in a typical DBQW structure (consisting of 20-Å AlAs, 60-Å $Al_{0.25}Ga_{0.75}As$, and 20-Å AlAs) tunnels out of the well through the barriers with the transmission energy spectrum shown in Fig. 2(b). Comparing this to the profile of

Fig. 2(a), the DBQW transmission is about four orders of magnitude higher for $E<0.235$ eV. This implies that the DBQW dark current at near-zero applied voltage is higher than that in the full barrier QW. The transmission does not immediately rise at 0.235 eV, but does so at 0.242 eV because the X-like barrier (0.332 eV) of the $Al_{0.25}Ga_{0.75}As$ middle layer (B_2) blocks the X-like state enhancement in the AlAs layer [see the band profile in Fig. 1(a)]; thus the electron has to tunnel through either the 0.242 eV Γ-band barrier or the 0.332 eV X-band barrier. The transmission peak feature at 0.273 eV (E_{X0}) is identified as a X-like quasibound state in the 20-Å AlAs layer (B_1). In $Al_{0.25}Ga_{0.75}As$, the Γ minimum is lower than the X minima, so that, in the energy range $0.242<E<0.332$ eV, most electrons travel over the Γ-band barrier, resulting in a high transmission probability. Above 0.332 eV, electrons may also tunnel via the X-like state in B_2, but the transmission does not increase significantly. Above 0.362 eV the total transmission increases by up to two orders of magnitude, due to the ΓX channel. The one-band transmission is not shown for the DBQW case [in either Figs. 2(b) or 2(d)] because it is similar to the ΓΓ transmission. This shows that electrons can tunnel through the DBQW barrier via the Γ-Γ-Γ path without any X-like state assistance. In the ΓΓ component, there are two significant peaks at 0.308 and 0.488 eV (which also appear in the one-band transmission) which correspond to the quasibound state in the B_2 Γ-like well. In fact, in order to minimize the interaction in each QW, the B_2 barrier layer must be thicker than 60 Å. Thus these peaks are characteristic of this particular structure, but similar features will be found in thicker B_2 barriers, but with peaks shifted to lower energy and with more states in the wider B_2 layer. The 60-Å B_2 layer is used here for illustrative purposes.

The DBQW barrier in Fig. 2(b) is the composite barrier between adjacent wells in the multiquantum well (MQW) structure, including a second B_1 layer belonging to the adjacent DBQW. The transmission for the single DBQW barrier has similar characteristics, with smooth ΓΓ transmission above the 0.242 eV step.

The transmission through the single finite barrier QW structure consisting of 80-Å AlAs, 45-Å GaAs, and 80-Å AlAs, shown in Fig. 2(c), was evaluated to investigate the quasibound levels. The transmission for the QW and its associated barrier [Figs. 2(c) and 2(a)] has similar features, and one Γ resonance state is observed as the significant peak at 0.118 eV ($E_{\Gamma 0}$). Some small peaks appear around 0.401 eV. A much greater transmission via X-like states in the thick AlAs barrier ($E>0.235$ eV) may be the reason for these unclear peaks. The other resonance peak at 0.401 ($E_{\Gamma 1}$) in the one-band transmission calculations correspond to the excited Γ-like quasibound state in the 45-Å GaAs well.

Theoretically, the transmission at the resonance peaks are close to unity, but for illustrative purposes the display energy resolution used in the transmission spectra is 0.002 eV, and thus the resonance peaks shown may not approach unity. Nevertheless, the energy resolution utilized in the transmission coefficient for the integration of the current-density calculation is of the order of 0.0001 eV or smaller depending on the transmission peak width for that particular case. In this manner, an accurate current density can be achieved. Figure 2(d) shows the transmission of the whole DBQW structure,

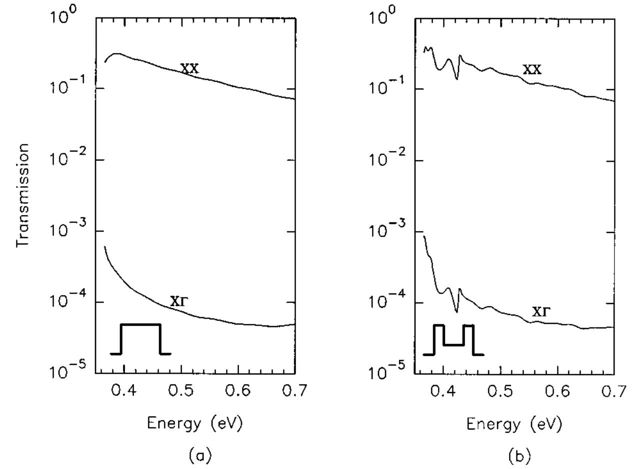

FIG. 3. X-valley incident electron transmission as a function of energy for (a) a 100-Å AlAs single barrier and (b) 20-Å AlAs, 60-Å $Al_{0.25}Ga_{0.75}As$, and 20-Å AlAs DBQW barriers. The insets show the Γ-barrier profiles.

consisting of 60-Å $Al_{0.25}Ga_{0.75}As$, 20-Å AlAs, 45-Å GaAs, 20-Å AlAs, and 60-Å $Al_{0.25}Ga_{0.75}As$. The $E_{\Gamma 0}$ and $E_{\Gamma 1}$ states at 0.118 and 0.431 eV from the GaAs well are slightly shifted, and are more significant than appear in Fig. 2(c). The E_{X0} quasibound state from the 20-Å AlAs X-like well are also shown at the same energy as in Fig. 2(b). For $E<0.235$ eV the DBQW transmission magnitude is about ten orders higher than that in the full barrier QW [Fig. 2(c)]. The DBQW transmission increases rapidly at the Γ-like $Al_{0.25}Ga_{0.75}As$ barrier (0.242 eV), and the ΓΓ transmission without X-like-state-assisted tunneling reaches approximately the same value as that in the ΓΓ transmission with X-like-state-assisted tunneling in Fig. 2(c). This indicates that, at low energy, the DBQW structure blocks electrons but allows Γ-valley electrons at high energy (i.e., photoelectrons) to pass through. This is the essential feature denoting improvement of signal: dark current ratio in a DBQW photoconductive element.

The X-valley incident electron transmission for the 100-Å full AlAs barrier and equivalent double barrier (20-Å AlAs, 60-Å $Al_{0.25}Ga_{0.75}As$, and 20-Å AlAs) are illustrated in Figs. 3(a) and 3(b), respectively. For $E>0.362$ eV, electrons can transfer into two final-state valleys, i.e., $X\Gamma$ and XX. The $X\Gamma$ contribution is three orders of magnitude lower than XX. For the full barrier case [Fig. 3(a)], the $X\Gamma$ and XX transmissions are equivalent to those in the Γ-valley incident electron case [ΓΓ and ΓX in Fig. 2(a), respectively]. The high transmission shows that electrons prefer to tunnel via X-like above-barrier states (X-X-Γ and X-X-X) rather than that via Γ-like below-barrier states (X-Γ-Γ and X-Γ-X). In contrast with the full barrier case, the Γ and X incident transmissions for the DBQW barrier [Figs. 2(b) and 3(b)] are considerably different. None of the resonant peaks which are associated with the Γ-like quasibound state in the B_2 layer are observed in either XX or $X\Gamma$ transmission. In addition, the ΓΓ transmission in Fig. 2(b) is slightly greater than $X\Gamma$. We can therefore conclude that the ΓΓ path is dominated by tunneling via Γ states in the B_2 layer, while the X-valley incident transmission is probably dominated by the electron traveling over the X state in the B_2 layer.

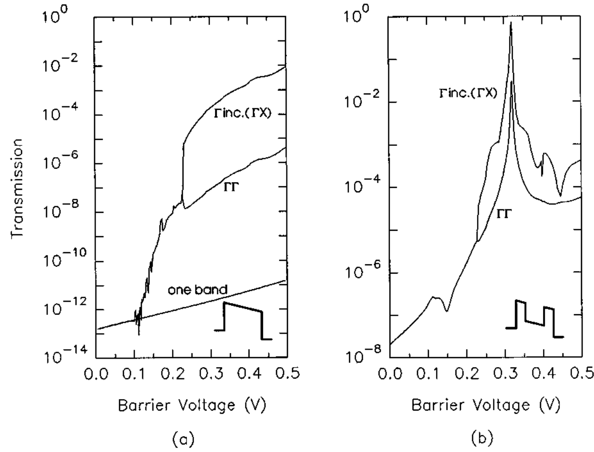

FIG. 4. Γ-valley incident electron transmission (Γinc.) including one-band, ΓΓ, and ΓX components at E_F as a function of barrier voltage for (a) a 100-Å AlAs single barrier and (b) 20-Å AlAs, 60-Å $Al_{0.25}Ga_{0.75}As$, and 20-Å AlAs DBQW barriers. The insets show the Γ barrier profiles at low-bias voltages.

B. Bias voltage structure

When a voltage is applied to the QW, the voltage drops partially in each barrier layer, and gradually lowers the potential barrier in proportion to the ratio between layer thickness and dielectric constant (since the normal component of displacement vector is conserved). The Γ-valley incident transmissions as a function of applied voltage for the 100-Å AlAs barrier [Fig. 4(a)] and for the 20-Å AlAs, 60-Å $Al_{0.25}Ga_{0.75}As$, and 20-Å AlAs DBQW barriers [Fig. 4(b)] are evaluated at E_F. In order to describe the dark current in the QWIP, we assume that electrons are mostly confined at and above the ground quasilevels of the DBQW ($E_{\Gamma 0}$), and tunnel out of the well through the barrier. With the Fermi-Dirac distribution of the two-dimensional electron gas in a 1×10^{18}-cm^{-3} doped well at 77 K, the Fermi energy (E_F) with an infinite well approximation is 15.5 meV above the $E_{\Gamma 0}$ level. This is used as a fixed electron energy in the transmission calculation [Figs. 4(a) and 4(b)].

As the potential is gradually lowered with increasing bias voltage, the whole transmission spectrum is obtained (Fig. 4) by varying the voltage of the fixed energy electron, and it can be related to the energy-dependent transmission (Fig. 2). At low voltage ($V<0.10$ V), as in Fig. 4(a), the full barrier E_F transmission increases slightly as in Fig. 2(a) for $E<0.235$ eV, in which the Γ-Γ-Γ channel alone dominates. At about 0.10 and 0.23 V [corresponding to 0.235 and 0.362 eV in Fig. 2(a)], the transmission increases because of the tunneling via the X valley in the AlAs barrier, and transferral into the X valley, respectively. These are not abrupt steps, as in Fig. 2(a), because the profiles of the well and barrier are modified by the applied voltage and are now trapezoidal in shape; thus the number of additional channels varies proportionally as the potential gradient changes. For example, at 0.10 V the bottom of the X-like well touches the E_F level, and electrons travel through the whole barrier via the Γ path. When the voltage increases further, some part of the X-like trapezoidal well potential falls below the E_F level, so electrons at E_F tunnel through the Γ path where the well potential is higher than E_F, and can go through the X channel, the bottom of which is lower than E_F. Therefore, in the AlAs barrier, electrons may go via the Γ band in some portion of the barrier, and via the X channel in the remainder. A series of peaks occurs in the transmission due to the X-like quasilevel in the trapezoidal well or in the asymmetric barrier.

The one-band transmission increases smoothly as the Γ-band potential barrier is gradually lowered when the voltage increases. At $V=0.3$ V, the one-band transmission calculation yields results four and eight orders of magnitude less than the ΓΓ and ΓX transmissions, respectively. This illustrates the substantial influence of the X band in the full indirect barrier QW.

For the DBQW structure shown in Fig. 4(b), the one-band transmission (not shown) approaches the ΓΓ transmission, since the pure Γ-band tunneling transmission is already high. As described in Sec. III A, the step occurs at 0.242 eV rather than at 0.235 eV in Fig. 2(b), because the electron is blocked by the X band of the B_2 barrier. The DBQW transmission also starts to increase at higher voltages, and the small peak at 0.12 V is associated with the X-like quasistate in the 20-Å AlAs layer (corresponding to the 0.273 eV state in the unbiased rectangular well). The resonant peak features of Γ-like quasibound state in B_2 at 0.308, 0.488, and 0.735 eV in Fig. 2(c) also show up significantly in the voltage-dependent transmission. For example, the 0.488-eV resonance level in the unbiased structure shifts to E_F and $E_{\Gamma 1}$ energy levels in the Γ-like B_2 trapezoidal well when voltages of 0.32 and 0.11 V are applied, respectively. The transmission peaks at these voltages are also shown in Fig. 4(b). These resonance voltages are shifted when the B_2 thickness increases; nevertheless the magnitude of the nonresonant transmission remains approximately unchanged. At low bias, the E_F electron transmission for DBQW is about five orders of magnitude higher than that for the full barrier, while for $V>0.23$ V the nonresonance total transmission in both structures becomes of the same order, although the magnitude of the ΓΓ component for the DBQW is one order greater than that in the full barrier.

The dark current as a function of applied voltage for the AlAs/GaAs QW and the $Al_{0.25}Ga_{0.75}As$/AlAs/GaAs DBQW with the same overall dimensions have been calculated and are shown in Figs. 5(a) and 5(b), respectively. Here we have selected a doping concentration of 1×10^{18} cm^{-3} in the GaAs well, and a temperature of 77 K. A mobility of 2000 cm^2/V s and saturation velocity of 5×10^6 cm/s were used to approximate the velocity at 77 K.[38] By integrating over the energy range with transmission weighted by the two-dimensional Fermi-Dirac distribution, the current has a similar characteristic to the E_F transmission (Fig. 4). However, the applied voltage is dropped across the well and barriers on both sides; thus, in order to approach the same voltage dropped across the barrier as in Fig. 4, a higher total voltage needs to be applied. No significant resonance current peak is observed in the full barrier QW, while there is an obvious resonance peak at 0.75 V in the DBQW. At low applied voltage, the DBQW current is lower for the full barrier by two orders of magnitude, but they become comparable at high-bias voltage.

The calculated current using ΓΓ transmission components (ΓΓ) is one and three orders lower than total current [Γ inc.(ΓX)] in DBQW and full barrier QW cases, respectively. The current in the one-band transmission is also

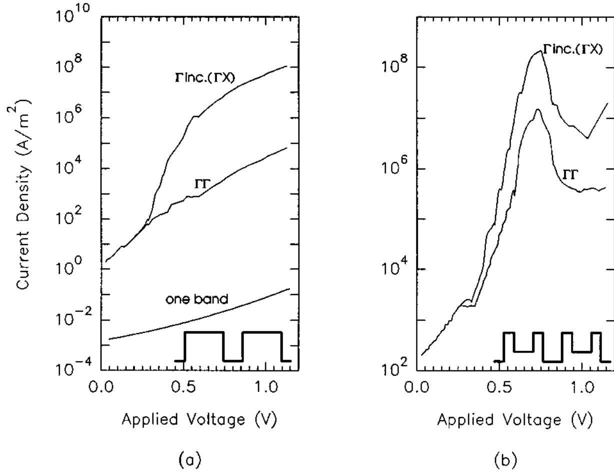

FIG. 5. Dark current density from ΓΓ, single-band, and total transmissions as a function of applied voltage at 77 K for (a) a AlAs/GaAs QW and (b) an $Al_{0.25}Ga_{0.75}As$/AlAs/GaAs DBQW. The insets show the unbiased Γ finite-barrier QW's.

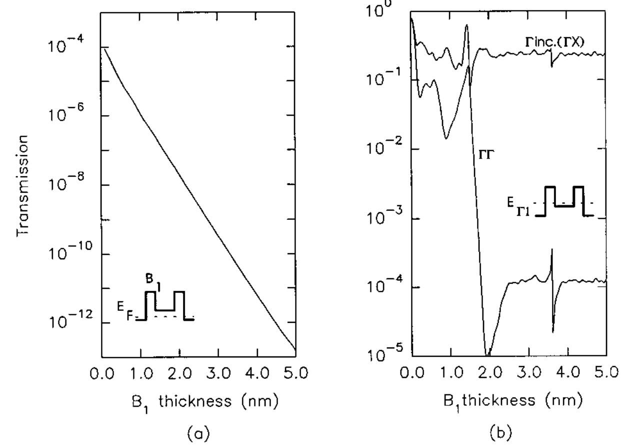

FIG. 6. Γ-valley incident electron transmission (Γinc.) as a function of AlAs barrier thickness at (a) E_F and (b) $E_{\Gamma 1}$ energy levels for an $Al_{0.25}Ga_{0.75}As$/AlAs/GaAs DBQW with zero-bias voltage. Γ-barrier profiles are shown in the insets.

shown for a full barrier QW (one band), and we find that for the DBQW it is in the same order as the ΓΓ transmission current. For the full barrier QW, however, it is about three orders of magnitude lower at low voltage. At high voltage, the one-band current is about five and eight orders of magnitude lower than the current formed using ΓΓ and total transmissions, respectively. This clearly shows that the X-band-assisted tunneling encourages much more dark current in the full indirect barrier QW. It also influences the dark current in the DBQW, but only at a high voltage.

In the above current calculation, we have assumed that the current is dominated by the electron in the single QW transmitting out of the well into the continuous state in the collector contact, and the current from the emitter is neglected. This can also be applied to the MQW case, in which the final state of the next well is assumed to be a continuous state as in the bound-to-continuous QWIP. This is valid only if the additional barrier is very thin, and if a quasibound state can be approximated as a continuous state. Under this assumption, the total current from the MQW is estimated by the number of wells times the single QW current, and also the equal division of the total applied voltage between QW's.

When the additional barrier (AlAs) becomes thick and the quasibound state becomes more tightly bound, sequential tunneling current may occur in the MQW. This current, below the voltage at which the resonance peak occurs, can be approximated by the current in the bound-to-bound QWIP, i.e., Eq. (1) in Ref. 44. The current can be approximated by assuming that it is directly proportional to the transmission probability at the Fermi-energy level [as shown in Fig. 4(b)]. Therefore, in both cases, the X-band electron has a small effect in the DBQW at low bias, but the effect increases as the voltage increases.

C. Additional barrier effects

In order to investigate further the effect of the additional barrier on electron transport in the DBQW, we have systematically varied the AlAs layer (B_1) thickness within a fixed total barrier thickness of 100 Å. The Γ incident transmissions at E_F and $E_{\Gamma 1}$ are shown in Figs. 6(a) and 6(b), respectively. With no bias voltage, the transmission at E_F originating from the ΓΓ electron path decays exponentially as the B_1 thickness increases [Fig. 6(a)]. Thus for pure Γ transmission, the DBQW B_1 and B_2 barriers can be regarded as a single barrier with an effective barrier height. When the ratio of B_1 and B_2 thicknesses increases, the effective barrier height also increases proportionally.

Figure 6(b) shows that, as B_1 thickness increases, the ΓΓ transmission component at $E_{\Gamma 1}$ decreases and becomes approximately constant after a certain B_1 thickness, while the ΓX component is almost constant over the barrier thickness range. This is caused by the X-like-state-assisted tunneling involving in the ΓΓ transmission for the thick B_1 layer structure, and in the ΓX transmission for over-the-barrier thickness ranges. In other words, for a thin B_1 barrier, an electron can easily tunnel through the B_1 barrier, so the pure Γ transmission dominates and decreases as B_1 thickness increases. The pure Γ transmission continuously decreases down to about 10^{-11} for a 50-Å B_1 structure [estimated by the one-band transmission of the full AlAs barrier in Fig. 2(a)]. Thus the ΓΓ transmission with X-like-state-assisted tunneling (about 10^{-4}) becomes dominant for the thick B_1 structure. The peak, appearing at the 15 Å B_1 barrier, corresponds to the Γ-like resonance state in the B_2 layer. The $E_{\Gamma 1}$ level is higher than any X-minima barrier, so electrons can comfortably be transmitted via the ΓX channel.

IV. CONCLUSION

Electron transport in the $Al_{0.25}Ga_{0.75}As$/AlAs/GaAs DBQW has been studied. The AlAs barrier layer thickness is systematically varied from the direct barrier $Al_{0.25}Ga_{0.75}As$/GaAs QW to DBQW, and then to the full indirect barrier AlAs/GaAs QW. The electron transmission out of the well through the various barriers via Γ- and/or X-like states, with and without bias voltage, was discussed in detail.

For 60-Å $Al_{0.25}Ga_{0.75}As$, 20-Å AlAs, and 45-Å GaAs DBQW structures, three Γ-like quasibound states at 0.118,

0.431, and 0.806 eV are observed. These levels are slightly shifted from those in the AlAs/GaAs QW. The response wavelength associated with the transition between the first two states is 3.9 μm. The excited resonant state in the full barrier QW is not clearly seen in the transmission because the Γ-confined electron transmission is very weak compared to tunneling via X-like states. The tunneling transmission for both Γ and X incident electrons via an X-like quasibound state is in the form of a peak, and transmission via X-like virtual above-barrier states increases in the form of a step function (to near unity); in other words, electrons in this channel are almost totally transmitted.

By varying the applied voltage, the fixed energy transmission can also give the whole spectrum, but the resonance level is slightly shifted because the electron is confined in a well which is trapezoidal rather than rectangular. When a voltage is applied, the potential is gradually lowered, and an electron in one layer may travel via Γ states in one portion of the slab, and transfer to X-like states in the remainder. This results in no abrupt step in the transmission as a function of voltage.

The dark current is simulated by confined ground-state electrons tunneling out of the well. We found that, at high-bias voltage, tunneling via X-like states may increase the current by a few orders of magnitude. The single-band calculations give the same magnitude as for tunneling via the ΓΓ channel in the DBQW structure, while the single-band current for the AlAs/GaAs QW is about four orders of magnitude lower than the current in X-like-state-assisted tunneling via the ΓΓ path. Tunneling via X-like states significantly affects the current in the full indirect barrier QW rather than that in DBQW. However, when the additional barrier thickness is also varied, we find that, in a very thin AlAs barrier (<20 Å), the excited-state electron is not blocked by the Γ-band barrier, and may give a high photocurrent without X-band assistance.

For multiquantum wells used in QWIP, in order to increase the photoelectron current, the applied voltage is equally dropped in all QW's so that only the current at small voltages is significant and the total current becomes the number of wells times the current from each well. The currents for both thin and thick additional barrier MQW structures are also estimated. The sequential tunneling current may be considered not only between Γ-like states but also transferring sequentially to different states in another well.

ACKNOWLEDGMENTS

We would like to acknowledge a grant from Australian Institute of Nuclear Science and Engineering (AINSE) for the use of the supercomputer at the Australian Nuclear Science and Technology Organization (ANSTO). This work is also supported by both the Australia Research Council (ARC) and the Australian International Development Assistance Bureau (AIDAB).

---

*Present address: Department of Physics, Faculty of Science, Mahidol University, Phaya Tai, Bangkok 10400, Thailand.

†Present address: Centre for Photovoltaics and Systems, School of Electrical Engineering, The University of New South Wales, NSW 2052, Australia.

[1] B. F. Levine, J. Appl. Phys. **74**, R1 (1993).

[2] B. F. Levine, A. Y. Cho, J. Walker, R. J. Malik, D. A. Kleinman, and D. L. Sivco, Appl. Phys. Lett. **52**, 1481 (1988).

[3] E. C. Larkins, H. Schneider, S. Ehret, J. Fleibner, B. Dischler, P. Koidl, and J. D. Ralston, IEEE Trans. Electron Dev. **41**, 511 (1994).

[4] H. Schneider, F. Fuchs, B. Dischler, J. D. Ralston, and P. Koidl, Appl. Phys. Lett. **58**, 2234 (1991).

[5] T. Osotchan, V. W. L. Chin, M. R. Vaughan, T. L. Tansley, and E. M. Goldys, Phys. Rev. B **50**, 2409 (1994).

[6] H. C. Liu, P. H. Wilson, M. Lamm, A. G. Steele, Z. R. Wasilewski, and J. Li, Appl. Phys. Lett. **64**, 475 (1994).

[7] M. Leroux, N. Grandjean, B. Chastaingt, C. Deparis, G. Neu, and J. Massies, Phys. Rev. B **45**, 11 846 (1992).

[8] B. Deveaud, D. Morris, A. Regreny, R. Planel, J. M. Gerard, M. R. X. Barros, and P. Becker, Semicond. Sci. Technol. **9**, 722 (1994).

[9] D. Landheer, H. C. Liu, M. Buchanan, and R. Stoner, Appl. Phys. Lett. **54**, 1784 (1989).

[10] P. M. Solomon, S. T. Wright, and C. Lanza, Superlatt. Microstruct. **2**, 521 (1986).

[11] E. E. Mendez, W. I. Wang, E. Calleja, and C. E. T. Goncalves da Silva, Appl. Phys. Lett. **50**, 1263 (1987).

[12] R. Beresford, L. F. Luo, W. I. Wang, and E. E. Mendez, Appl. Phys. Lett. **55**, 1555 (1989).

[13] Z. Othaman, A. K. Giem, S. J. Bending, R. T. Syme, and R. S. Smith, Semicond. Sci. Technol. **8**, 1483 (1993).

[14] Y. Carbonneau, J. Beerens, L. A. Cury, H. C. Liu, and M. Buchanan, Appl. Phys. Lett. **62**, 1955 (1993).

[15] P. J. Price, Surf. Sci. **196**, 394 (1988).

[16] H. C. Liu, Appl. Phys. Lett. **51**, 1019 (1987).

[17] J. A. Stovneng and P. Lipavsky, Phys. Rev. B **49**, 16 494 (1994).

[18] T. B. Boykin, J. P. A. van der Wagt, and J. S. Harris, Jr., Phys. Rev. B **43**, 4777 (1991).

[19] N. A. Cade, S. H. Parmar, N. R. Couch, and M. J. Kelly, Solid State Commun. **64**, 283 (1987).

[20] R. E. Carnahan, K. P. Martin, R. J. Higgins and G. Park, E. Wolak, K. L. Lear, and J. S. Harris, Jr., Semicond. Sci. Technol. **9**, 500 (1994).

[21] A. R. Bonnefoi, T. C. McGill, and R. D. Burnham, Phys. Rev. B **37**, 8754 (1988).

[22] K. V. Rousseau, K. L. Wang, and J. N. Schulman, Appl. Phys. Lett. **54**, 1341 (1989).

[23] T.-H. Shieh and S.-C. Lee, Appl. Phys. Lett. **63**, 3350 (1993).

[24] Y. Zhang, X. Yang, W. Liu, P. Zhang, and D. Jiang, Appl. Phys. Lett. **65**, 1148 (1994).

[25] S. N. Grinyaev, G. F. Karavaev, and V. N. Chernyshov, Fiz. Tekh. Poluprovodn. **28**, 1303 (1994) [Sov. Phys. Semicond. **28**, 784 (1994)].

[26] D. Y. K. Ko and J. C. Inkson, Phys. Rev. B **38**, 12 416 (1988).

[27] G. Edwards and J. C. Inkson, Semicond. Sci. Technol. **9**, 310 (1994).

[28] D. Y. K. Ko and J. C. Inkson, Phys. Rev. B **38**, 9945 (1988).

[29] A. C. Marsh, IEEE J. Quantum Electron. **QE-23**, 371 (1987).

[30] S. Brand and D. T. Hughes, Semicond. Sci. Technol. **2**, 607 (1987).

[31] T. B. Boykin and J. S. Harris, Jr., J. Appl. Phys. **72**, 988 (1992).

[32] D. Z.-Y. Ting and T. C. McGill, Phys. Rev. B **47**, 7281 (1993).
[33] J. P. Cuypers and W. van Haeringen, Phys. Rev. B **47**, 10 310 (1993).
[34] J. B. Xia, Phys. Rev. B **41**, 3117 (1990).
[35] T. Ando and H. Akera, Phys. Rev. B **40**, 11 619 (1989).
[36] E. S. Hellman and J. S. Harris, Jr., Superlatt. Microstruct. **3**, 167 (1987).
[37] T. Osotchan, V. W. L. Chin, and T. L. Tansley, Phys. Rev. B **52**, 5202 (1995).
[38] K. M. S. V. Bandara, B. F. Levine, R. E. Leibenguth, and M. T. Asom, J. Appl. Phys. **74**, 1826 (1993).
[39] A. Baldereschi, E. Hess, K. Maschke, H. Neumann, and K.-R. Schulze, J. Phys. C **10**, 4709 (1977).
[40] S. Adachi, J. Appl. Phys. **58**, R1 (1985).
[41] H. J. Drouhin, C. Hermann, and G. Lampel, Phys. Rev. B **31**, 3859 (1985).
[42] B. Monemar, Phys. Rev. B **8**, 5711 (1973).
[43] G. Danan, B. Etienne, F. Mollot, and R. Planel, Phys. Rev. B **35**, 6207 (1987).
[44] K. K. Choi, B. F. Levine, R. J. Malik, J. Walker, and C. G. Bethea, Phys. Rev. B **35**, 4172 (1987).